

## Synthesis and Cavity Size Effect of Pd-Containing Macrocycle Catalyst for Efficient Intramolecular Hydroamination of Allylurethane

Masahiro Ogawa,<sup>†</sup> Masaki Nagashima,<sup>†</sup> Hiromitsu Sogawa,<sup>†</sup> Shigeki Kuwata,<sup>‡</sup> and Toshikazu Takata<sup>\*,†,§</sup><sup>†</sup>Department of Organic and Polymeric Materials and <sup>‡</sup>Department of Applied Chemistry, Tokyo Institute of Technology, O-okayama, Meguro-ku, Tokyo 152-8552, Japan<sup>§</sup>Advanced Catalytic Transformation for Carbon Utilization (ACT-C), JST, O-okayama, Meguro-ku, Tokyo 152-8552, Japan

## Supporting Information

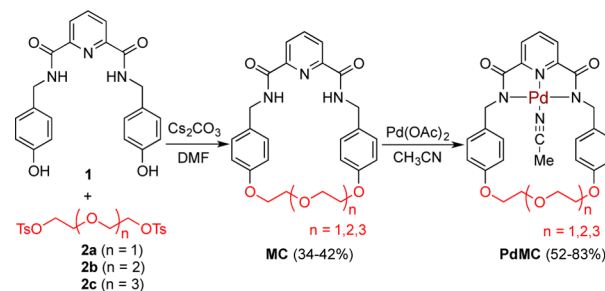
**ABSTRACT:** Palladium-containing macrocycle catalysts (PdMCs) with different ring sizes ranging from 24 to 30 members were synthesized. The intramolecular hydroamination of an allylurethane (AU) catalyzed by PdMCs proceeded efficiently to afford the corresponding oxazolidinone (OZ) in 95% isolated yield. The dependence of the hydroamination of AU to OZ on the cavity size indicated that the reaction rate was clearly controlled by both substrate uptake and product release steps.



Development of supramolecular catalysts exhibiting elegant and efficient catalytic activity is an interesting and attractive topic for chemists.<sup>1</sup> Among those supramolecular catalysts, macrocycle catalysts represented by Cu-modified  $\beta$ -cyclodextrins<sup>2</sup> are characterized by facile preparation of a flexible framework and easy cavity control through the choice of reaction type. Because of the specific space for reactions around the metals in these catalysts, the catalysts often exhibit size-selective catalysis.<sup>3–5</sup> Nolte, Rowan, and co-workers performed detailed studies of metalloporphyrin-containing macrocycles that effectively catalyze the epoxidation of polymeric alkenes via a pseudorotaxane intermediate. This reaction mimics the reaction mode of  $\lambda$ -exonuclease,<sup>6</sup> which also proceeds via a pseudorotaxane intermediate with DNA. Meanwhile, we reported the intramolecular cyclization of allylurethanes to oxazolidinones catalyzed by a Pd-tethering macrocycle catalyst (PdMC)<sup>7</sup> after our finding of a similar transformation within a rotaxane molecule with four allylurethane moieties in the axle component.<sup>7b</sup> Interestingly, this catalytic hydroamination of allylurethanes with pyridyl moieties proceeds only when the allylurethane can form a pseudorotaxane complex with PdMC, suggesting that the reaction takes place in the catalyst cavity.<sup>7</sup> Although such macrocycle catalysts are expected to have a potential utility as a highly active and selective catalyst, to the best of our knowledge the characteristic features of their catalysis have not yet been investigated. We have studied the functions of PdMCs and recently found a unique catalysis specific to their macrocyclic structures that is disclosed in this paper. This PdMC-catalyzed intramolecular hydroamination of allylurethane depends largely upon the cavity size of PdMC, which affected not only the initial complexation with substrate followed by the Pd-catalyzed hydroamination but also the elimination of the product from the cavity.

PdMCs with three different ring sizes were prepared via a two-step reaction starting from the pincer-type ligand (**1**), as illustrated in Scheme 1 and according to our previously

## Scheme 1. Synthesis of Macrocycle Catalysts (PdMCs)



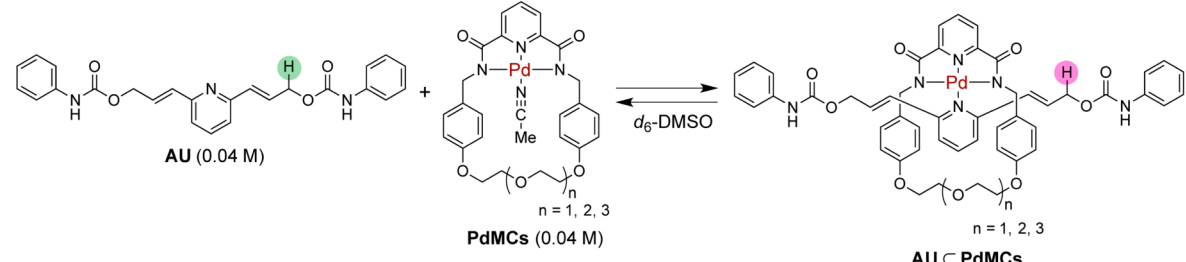
reported method for PdMC30.<sup>7a</sup> Namely, initial macrocycle formation from pyridine bisamide ligand **1** and an oligo(ethylene glycol) (MC24, MC27, or MC30) was followed by palladium insertion into the cavity of the MCs using palladium(II) diacetate to afford the corresponding PdMCs in good yields. The structures of PdMCs were determined using <sup>1</sup>H NMR, MALDI-TOF MS and X-ray crystal structure analyses.

The association constant ( $K_a$ ) between PdMC and a pyridine-containing bis(allylurethane) (AU) was evaluated by <sup>1</sup>H NMR spectra in *d*<sub>6</sub>-DMSO at various temperatures (from 40 to 120 °C), as shown in Table 1.<sup>8</sup> The formation of a 1:1 inclusion complex (AU ⊂ PdMC) was readily confirmed by the

Received: February 6, 2015

Published: March 17, 2015

Table 1. Complexation between PdMCs and AU



$K_a$ ( $M^{-1}$ ) <sup>a,b</sup>	40 °C	60 °C	80 °C	100 °C	120 °C
PdMC24	0	0	0	0	0
PdMC27	150 ± 59	110 ± 40	65 ± 15	47 ± 6	22 ± 6
PdMC30	880 ± 210	460 ± 60	190 ± 10	120 ± 10	59 ± 6

<sup>a</sup>Estimated by <sup>1</sup>H NMR spectrum. <sup>b</sup>[PdMCs] = [AU] = 0.04 M.

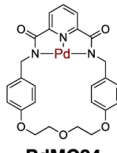
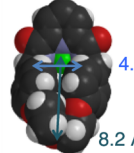
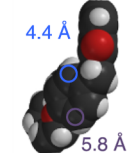
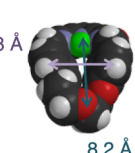
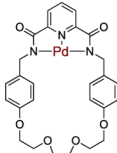
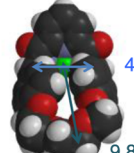
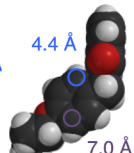
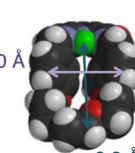
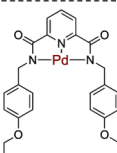
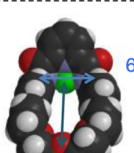
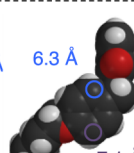
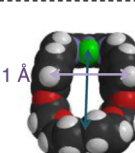
upfield shift of the methylene proton peaks of AU (Figure S1). This result strongly suggested the formation of a pseudorotaxane complex on the basis of the similarity of NMR spectra to those obtained in our previous study.<sup>7b</sup> The thermodynamic parameters for pseudorotaxane formation were also determined by van't Hoff plot in *d*<sub>6</sub>-DMSO (Figure S2 and Table S1).

Although no complex was formed with PdMC24, complexes were obtained with PdMC27 and PdMC30, which had larger cavity sizes. As can be seen in Table 1, AU ⊂ PdMC30 exhibited a larger  $K_a$  than AU ⊂ PdMC27 at all temperatures, indicating that AU ⊂ PdMC30 is more stable than AU ⊂ PdMC27. Clear MALDI-TOF-MS peaks corresponding to AU ⊂ PdMC27 ( $m/z$  1047.77 [M + Na]<sup>+</sup>,  $m/z$  1047.25 calcd for C<sub>52</sub>H<sub>50</sub>N<sub>6</sub>O<sub>10</sub>Pd) and AU ⊂ PdMC30 ( $m/z$  1091.63 [M + Na]<sup>+</sup>,  $m/z$  1091.28 calcd for C<sub>54</sub>H<sub>54</sub>N<sub>6</sub>O<sub>11</sub>Pd) were observed.

The cavity sizes of PdMCs have been estimated by X-ray analysis of the acetonitrile complexes or their derivative (Table 2). The structural data revealed that the distances between the Pd atoms and oxyethylene portions of PdMC24, PdMC27, and PdMC30 were ca. 8.2, 9.8, and 9.9 Å,<sup>7b</sup> respectively. The cavity-sizes clearly increased as the length of the oxyethylene spacer increased, as expected. Furthermore, two face-to-face benzene rings in PdMC24 were twisted to shrink its cavity width (5.8 Å), which is likely due to the shorter spacer length, which was not observed in PdMC27 (7.0 Å) or PdMC30 (7.1 Å). This constrained structure should control the formation of the pseudorotaxane-type complex with AU.

Next, a solution of AU, triethylamine (200 mol %), and PdMC27 (20 mol %) in *d*<sub>6</sub>-DMSO was heated at 80 °C for 95 h to give the corresponding hydroamination product (OZ) in 95% isolated yield with a diastereomer ratio of ca. 50:50. With PdMC30, the yield of OZ was 72%, and no OZ was obtained with PdMC24. The catalytic activity of PdMC was investigated by monitoring the <sup>1</sup>H NMR spectral changes during the reaction of AU in the presence of PdMC (20 mol %) and triethylamine in DMSO (Figure 1). No changes in the <sup>1</sup>H NMR spectrum were observed with PdMC24, even after 57 h, which was in contrast to PdMC27 and PdMC30; the intramolecular hydroamination of AU to OZ with these catalysts readily occurred with 100% conversion, as shown in Figure 1a. These results clearly reveal that the complexation of AU with PdMC plays a key role in the reaction. Interestingly, the initial rate of the reaction with PdMC30 was greater than that with PdMC27, although the reaction with PdMC30 took longer to reach completion than the reaction with PdMC27.<sup>9</sup>

Table 2. Cavity Sizes for PdMCs Estimated by X-ray Analysis

PdMCs <sup>a</sup>	back	side	down
 PdMC24	 8.2 Å	 4.4 Å 5.8 Å	 5.8 Å 8.2 Å
 PdMC27 <sup>b</sup>	 9.8 Å	 4.4 Å 7.0 Å	 7.0 Å 9.8 Å
 PdMC30	 9.9 Å	 6.3 Å 7.1 Å	 7.1 Å 9.9 Å

<sup>a</sup>Calculated from the crystal structures of the acetonitrile complexes.

<sup>b</sup>Structural parameters have been estimated from the crystal structure of a cyclic tetrameric derivative without acetonitrile ligands. Averaged values in the four crystallographically independent units are shown. See Supporting Information for details.

The time–conversion curves clearly indicate two different reaction stages (early and late). Considering all of the above-described results, a plausible reaction mechanism for the PdMC-catalyzed hydroamination of AU was proposed and is presented in Scheme 2.

The initial equilibrium formation of a pseudorotaxane complex between PdMC and AU is followed by the Pd-catalyzed hydroamination of one allylurethane moiety of AU. Successive hydroamination of the remaining allylurethane moiety proceeds with retention of the pseudorotaxane structure. Final PdMC elimination from the product–PdMC complex (OZ ⊂ PdMC) concludes a successful reaction cycle. Because no monohydroaminated product was detected in the <sup>1</sup>H NMR, the second hydroamination must be faster than the first one. In fact, the faster reaction with PdMC30 versus PdMC27 can be explained if the rate-limiting step is the initial monohydroamination from AU ⊂ PdMC (see the difference in

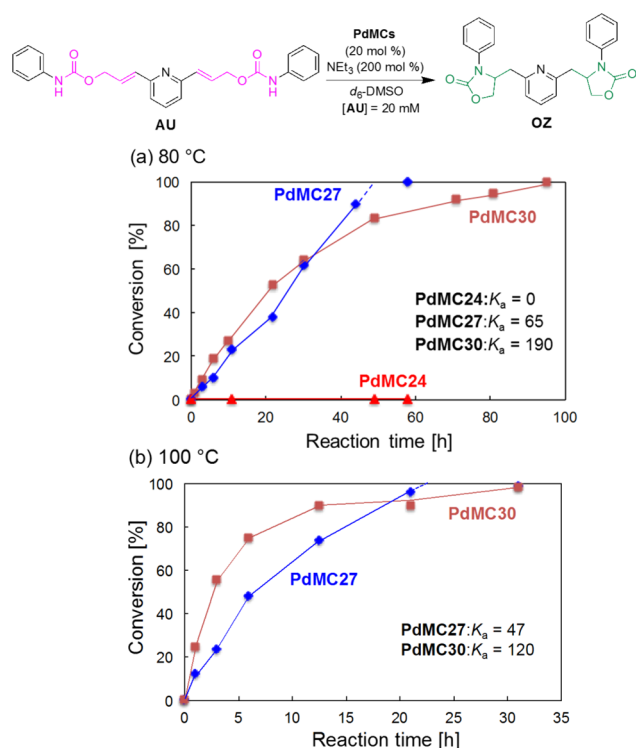
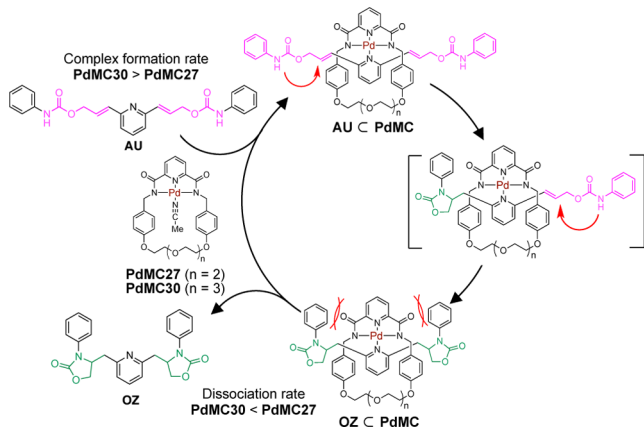


**Figure 1.** Time–conversion curves for the intramolecular hydroamination of AU catalyzed by PdMCs at (a) 80 and (b) 100 °C.

**Scheme 2. Plausible Reaction Mechanism for the Intramolecular Hydroamination of AU Catalyzed by PdMC**



$K_a$  values in Table 1). In addition, the faster completion of the reaction with PdMC27 can be accounted for if OZ < PdMC dissociates more rapidly to regenerate PdMC, which can be attributed to greater steric strain. This conclusion is supported by previous results obtained for PdMC30, which cannot translate over the two oxazolidinone moieties formed in the axial positions because of the bulkiness in the rotaxane system.<sup>7b</sup> Next, to examine the complexation between OZ and PdMCs, the catalysts were each mixed with OZ under various conditions. Interestingly, neither PdMC27 nor PdMC30 formed a complex with OZ in d<sub>6</sub>-DMSO at 25–100 °C. This result also supports the conclusion that the rate of the reaction with PdMC27 in the latter period does not decrease significantly, even though the concentration of substrate AU is lower.

To verify our proposed mechanism, density functional theory (DFT) calculations were performed using Gaussian 09.<sup>10</sup> The geometries of AU, OZ, PdMCs, AU < PdMCs, and OZ < PdMCs were optimized without any constraints using DFT method at B3LYP/lanl2dz levels in the presence of DMSO.<sup>11</sup> The initial geometries of PdMCs and their derivatives were determined or estimated using the results from the X-ray structure analyses. Figure 2 summarizes the relative energy

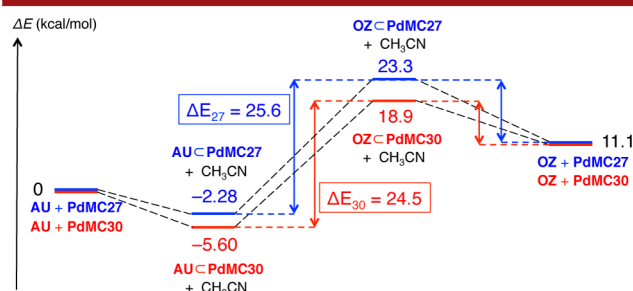


**Figure 2.** Relative energies for various intermediate structures involved in the PdMC-catalyzed intramolecular hydroamination of AU, for PdMCs with different cavity sizes. The energy values for AU + PdMC27 (−2 103 116.267 kcal/mol) and AU + PdMC30 (−2 199 643.318 kcal/mol) were calculated at the B3LYP/lanl2dz levels and set to zero for the PdMC27 and PdMC30 derivatives, respectively.

values for each conformation. The energy values for AU < PdMCs are lower than the totals of the individual energy values for AU and the corresponding PdMCs. Furthermore, AU < PdMC30 is more stable than AU < PdMC27, being consistent with the actual  $K_a$  values (Table 1). Meanwhile, the relative energy increases dramatically for OZ < PdMCs. Notably, because the energies are even higher than the total values for OZ and PdMCs, PdMCs can form complexes with AU remaining in the reaction mixture immediately after dissociation of OZ < PdMC intermediate. In addition, the difference in the relative energies for AU < PdMC and OZ < PdMC intermediates increases for PdMC27 ( $\Delta E_{27} - \Delta E_{30} = 1.1$  kcal/mol), as does the difference for OZ < PdMC and OZ + PdMC (4.4 kcal/mol). The lower the concentration of AU or AU < PdMC, the larger the contribution of the dissociation of OZ < PdMC to the reaction rate. These calculated results are in good agreement with the experimental results, including the unusual acceleration at the latter reaction stage and the proposed mechanism.

Note that if the proposed mechanism is correct then an increase in both the reaction temperature and catalyst concentration should affect the reaction profile, i.e., reduce the importance of the OZ < PdMC dissociation step. This assumption was confirmed: when the reaction was performed at 100 °C, only a slight difference in the completion time was observed for the catalysts with different ring sizes (Figure 1b). Namely, the difference in the energy differences  $\Delta E_{30}$  and  $\Delta E_{27}$  was diminished, leading to a reduction in the difference in the reaction rates for PdMC30 and PdMC27. Meanwhile, when the PdMC concentration was increased to 40 mol % (Figure 3), the reaction proceeded more rapidly than that with 20 mol % (Figure 1a), and the reaction with PdMC30 reached completion sooner than that with PdMC27. Thus, a high catalyst concentration appears to weaken the acceleration effect observed with 20 mol % PdMC27 because the reaction is complete before the effect (i.e., that PdMC27 was eliminated



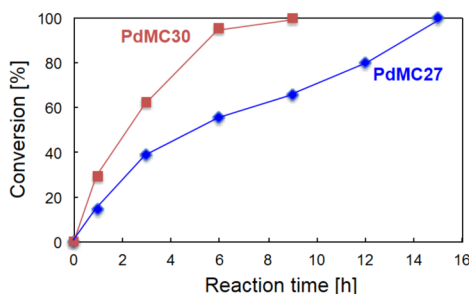


**Figure 3.** Time–conversion curves for the hydroamination of AU catalyzed by PdMC27 and PdMC30 (40 mol %) in  $d_6$ -DMSO at 80 °C.

from OZ faster than PdMC30 because of the larger steric hindrance (Scheme 2)) can distinctly emerge. The predicted experimental results obtained here indicate that the selection of macrocycle catalysts with appropriate cavity sizes is crucial for reactions that proceed via pseudorotaxane intermediates.

In this study, Pd-containing macrocycle (PdMC) complexes with three different cavity sizes were prepared and characterized. In addition, PdMCs with an appropriate cavity size efficiently catalyzed the intramolecular hydroamination of AU once incorporated into their cavities. Building on our previous report on the size effect of substrates,<sup>7b</sup> the results obtained in the present study clarified the importance of the cavity size of the catalysts. The current results also provide further valuable insight into catalyst structure design.

## ■ ASSOCIATED CONTENT

### Supporting Information

Experimental procedures and analytical and spectroscopic data for all new compounds. This material is available free of charge via the Internet at <http://pubs.acs.org>.

## ■ AUTHOR INFORMATION

### Corresponding Author

\*E-mail: [ttakata@polymer.titech.ac.jp](mailto:ttakata@polymer.titech.ac.jp).

### Notes

The authors declare no competing financial interests.

## ■ ACKNOWLEDGMENTS

This work was financially supported by the ACT-C program of JST, a Grant-in-Aid for Scientific Research from the Ministry of Education, Culture, Sports, Science, and Technology, Japan (no. 23245031).

## ■ REFERENCES

- (1) (a) van Dongen, S. F.; Cantekin, S.; Elemans, J. A.; Rowan, A. E.; Nolte, R. J. *Chem. Soc. Rev.* **2014**, *43*, 99–122. (b) Zarra, S.; Wood, D. M.; Roberts, D. A.; Nitschke, J. R. *Chem. Soc. Rev.* **2015**, *44*, 419–432. (c) Raynal, M.; Ballester, P.; Vidal-Ferran, A.; van Leeuwen, P. W. *Chem. Soc. Rev.* **2014**, *43*, 1660–1733. (d) Raynal, M.; Ballester, P.; Vidal-Ferran, A.; van Leeuwen, P. W. *Chem. Soc. Rev.* **2014**, *43*, 1734–1787. (e) Dong, Z.; Luo, Q.; Liu, J. *Chem. Soc. Rev.* **2012**, *41*, 7890–7908. (f) Friscic, T. *Chem. Soc. Rev.* **2012**, *41*, 3493–3510. (g) Hapiot, F.; Tilloy, S.; Monflier, E. *Chem. Rev.* **2006**, *106*, 767–781. (h) Vriezema, D. M.; Comellas Aragones, M.; Elemans, J. A.; Cornelissen, J. J.; Rowan, A. E.; Nolte, R. J. *Chem. Rev.* **2005**, *105*, 1445–1489. (i) Marchetti, L.; Levine, M. *ACS Catal.* **2011**, *1*, 1090–1118. (j) Murakami, Y.; Kikuchi, J.; Hisaeda, Y.; Hayashida, O. *Chem. Rev.* **1996**, *96*, 721–758. (k) Suzuki, Y.; Shimada, K.; Chihara, E.;

- Saito, T.; Tsuchido, Y.; Osakada, K. *Org. Lett.* **2011**, *13*, 3774–3777.
- (l) Lee, T.; Kalenius, E.; Alexandra, I. L.; Assaf, K. I.; Kuhnert, N.; Grün, C. H.; Jänis, J.; Scherman, O. A.; Nau, W. M. *Nat. Chem.* **2013**, *5*, 376–382. (m) Ogoshi, T.; Ueshima, N.; Yamagishi, T. *Org. Lett.* **2013**, *15*, 3742–3745. (n) Huang, F.; Zakharov, L. N.; Rheingold, A. L.; Khorassani, M. A.; Gibson, H. W. *J. Org. Chem.* **2005**, *70*, 809–813.
- (2) Breslow, R.; Overman, L. E. *J. Am. Chem. Soc.* **1970**, *92*, 1075–1077.
- (3) Lee, L. C.; Zhao, Y. *Org. Lett.* **2012**, *14*, 784–787.
- (4) Horike, S.; Dinca, M.; Tamaki, K.; Long, J. R. *J. Am. Chem. Soc.* **2008**, *130*, 5854–5855.
- (5) Yang, H.; Chong, Y.; Li, X.; Ge, H.; Fan, W.; Wang, J. *J. Mater. Chem.* **2012**, *22*, 9069–9076.
- (6) Kovall, R.; Matthews, B. W. *Science* **1997**, *277*, 1824–1827.
- (7) (a) Furusho, Y.; Matsuyama, T.; Takata, T.; Moriuchi, T.; Hirao, T. *Tetrahedron Lett.* **2004**, *45*, 9593–9597. (b) Miyagawa, N.; Watanabe, M.; Matsuyama, T.; Koyama, Y.; Moriuchi, T.; Hirao, T.; Furusho, Y.; Takata, T. *Chem. Commun.* **2010**, *46*, 1920–1922.
- (8) Nielsen, M. B.; Jeppesen, J. O.; Lau, J.; Lomholt, C.; Damgaard, D.; Jacobsen, J. P.; Becher, J.; Stoddart, J. F. *J. Org. Chem.* **2001**, *66*, 3559–3563.
- (9) The reaction orders for hydroamination of AU were evaluated. As results, the reaction orders using PdMC27 and PdMC30 at 100 °C and PdMC30 at 80 °C were assumed to be almost one. The reaction with PdMC27 at 80 °C did not fit a first-order equation. This result also suggested the unique catalytic activity of PdMC27.
- (10) Frisch, M. J.; Trucks, G. W.; Schlegel, H. B.; Scuseria, G. E.; Robb, M. A.; Cheeseman, J. R.; Scalmani, G.; Barone, V.; Mennucci, B.; Petersson, G. A.; Nakatsuji, H.; Caricato, M.; Li, X.; Hratchian, H. P.; Izmaylov, A. F.; Bloino, J.; Zheng, G.; Sonnenberg, J. L.; Hada, M.; Ehara, M.; Toyota, K.; Fukuda, R.; Hasegawa, J.; Ishida, M.; Nakajima, T.; Honda, Y.; Kitao, O.; Nakai, H.; Vreven, T.; Montgomery, J. A.; Peralta, Jr., J. E.; Ogliaro, F.; Bearpark, M.; Heyd, J. J.; Brothers, E.; Kudin, K. N.; Staroverov, V. N.; Keith, T.; Kobayashi, R.; Normand, J.; Raghavachari, K.; Rendell, A.; Burant, J. C.; Iyengar, S. S.; Tomasi, J.; Cossi, M.; Rega, N.; Millam, J. M.; Klene, M.; Knox, J. E.; Cross, J. B.; Bakken, V.; Adamo, C.; Jaramillo, J.; Gomperts, R.; Stratmann, R. E.; Yazyev, O.; Austin, A. J.; Cammi, R.; Pomelli, C.; Ochterski, J. W.; Martin, R. L.; Morokuma, K.; Zakrzewski, V. G.; Voth, G. A.; Salvador, P.; Dannenberg, J. J.; Dapprich, S.; Daniels, A. D.; Farkas, O.; Foresman, J. B.; Ortiz, J. V.; Cioslowski, J.; Fox, D. J. *Gaussian 09*, revision C.01; Gaussian, Inc.: Wallingford CT, 2010.
- (11) (a) Becke, A. D. *J. Chem. Phys.* **1993**, *98*, 5648–5652. (b) Parr, R. G.; Yang, W. *Density-Functional Theory of Atoms and Molecules*; Oxford University Press: Oxford, U.K., 1989. (c) Lee, C. T.; Yang, W. T.; Parr, R. G. *Phys. Rev. B* **1988**, *37*, 785–789. (d) Hay, P. J.; Wadt, W. R. *J. Chem. Phys.* **1985**, *82*, 270–283. (e) Wadt, W. R.; Hay, P. J. *J. Chem. Phys.* **1985**, *82*, 284–298. (f) Hay, P. J.; Wadt, W. R. *J. Chem. Phys.* **1985**, *82*, 299–310. (g) Dunning, T. H., Jr.; Hay, P. J. In *Modern Theoretical Chemistry*; Schaefer, H. F., III, Ed.; Plenum: New York, 1976; Vol. 3, pp 1–28.